

Dwarf Nova Oscillations and Quasi-Periodic Oscillations in Cataclysmic Variables: II. A Low Inertia Magnetic Accretor Model.

Brian Warner[★] and Patrick A. Woudt[†]

Department of Astronomy, University of Cape Town, Private Bag, Rondebosch 7700, South Africa

ABSTRACT

The Dwarf Nova Oscillations observed in Cataclysmic Variable (CV) stars are interpreted in the context of a Low Inertia Accretor model, in which accretion on to an equatorial belt of the white dwarf primary causes the belt to vary its angular velocity. The rapid deceleration phase is attributed to propeller. Evidence that temporary expulsion rather than accretion of gas occurs during this phase is obtained from the large drop in EUV flux.

We show that the QPOs are most probably caused by a vertical thickening of the disc, moving as a travelling wave near the inner edge of the disc. This alternately obscures and ‘reflects’ radiation from the central source, and is visible even in quite low inclination systems. A possible excitation mechanism, caused by winding up and reconnection of magnetic field lines, is proposed.

We apply the model, deduced largely from VW Hyi observations, to re-interpret observations of SS Cyg, OY Car, UX UMa, V2051 Oph, V436 Cen and WZ Sge. In the last of these we demonstrate the existence of a 742 s period in the light curve, arising from obscuration by the travelling wave, and hence show that the two principal oscillations are a DNO and its reprocessed companion.

Key words: accretion, accretion discs – novae, cataclysmic variables – stars: oscillations – stars: individual: VW Hyi, SS Cyg, OY Car, UX UMa, V2051 Oph, V436 Cen, WZ Sge

1 INTRODUCTION

In an earlier paper (Woudt & Warner 2002; hereafter Paper I) we have presented and analysed observations of Dwarf Nova Oscillations (DNOs) and Quasi-Periodic Oscillations (QPOs) in the dwarf nova VW Hyi, to which we added an overview of DNOs and QPOs in other dwarf novae and in nova-like variables.

The richness of the phenomenology, in which similarities as well as gross differences in behaviour are discernable among the various stars, suggests that although a unifying model may exist, there must be at least one parameter that takes different values in different systems. In this paper we explore such a model – the Low Inertia Magnetic Accretor (LIMA), which is described in Section 2. In Section 3 we consider the suggestion that QPOs are the result of vertical oscillations in the accretion disc. Section 4 applies the

LIMA and disc oscillation models to interpret observations of systems other than VW Hyi, including the EUV and X-ray DNOs seen in SS Cyg, and in Section 5 we conclude with a list of the principal observations and interpretative results from the two papers, and add some general remarks.

2 THE LOW INERTIA MAGNETIC ACCRETOR

The model of DNOs used and developed here originates in the suggestion of Paczynski (1978) that matter accreted during a dwarf nova outburst would generate a rapidly rotating equatorial belt on the white dwarf primary. Any magnetic field anchored in this belt, and at least partially controlling accretion near the primary, would result in accretion curtains and shocks in the same manner as in the standard intermediate polar (IP) structure (e.g. Warner 1995a) but with a variable frequency as the belt is spun up during the high accretion phase and decelerates afterwards. Any primary whose intrinsic field is too weak (less than about 10^5

[★] email: warner@physci.uct.ac.za

[†] email: pwoudt@artemis.uct.ac.za

G: see Section 2.3) to enforce solid body rotation will be subject to such a process, but only those systems in which the field is, or becomes (through shearing by the differential rotation), strong enough to control some accretion will show DNOs by this process. The approach, therefore, should be seen as an extension of the IP model to lower field strengths and is compatible with the essentially mono-periodic nature (plus reprocessing sidebands) of the IP and DNO modulations.

This model, which results from the low inertia of the equatorial belt, has been reviewed and extended by Warner (1995b). Since then, additional observational evidence has accrued. HST spectroscopy obtained after a superoutburst of VW Hyi indicates the existence of a white dwarf primary with $\log g = 8.0$, $v \sin i = 300 \text{ km s}^{-1}$ and surface temperature 22 500 K one day after outburst, cooling to 20 500 K 9 days later, together with an equatorial belt maintaining a temperature $\sim 30\,000 \text{ K}$ and $v \sin i \sim 3350 \text{ km s}^{-1}$ for the full ten days after outburst (Sion et al. 1996; see also Gänsicke & Beuermann 1996). The rotation rate of the equatorial belt is close to Keplerian, and the deduced gravitational acceleration for that component is $\log g = 6.0$, indeed implying dominantly centrifugal support. For an accreted belt mass of $2 \times 10^{-10} M_{\odot}$ the temperature of the belt is in agreement with the sequence of models computed by Sion (1995). The observations are not sufficiently precise to exclude some deceleration of the equatorial belt in the post-outburst phase.

An equatorial accretion belt has also been deduced for U Gem (Cheng et al. 1997a; Long et al. 1993), decreasing in temperature and area for some weeks after outburst. Comparisons of the observed cooling of the white dwarf primaries after superoutbursts of WZ Sge and AL Com show agreement with models only if the latter include a persistent fast rotating equatorial belt (Szkody et al. 1998).

A possible detection of the effects of magnetic channeling of accretion flow onto the primary in VW Hyi from a truncated disc during a superoutburst is given by Huang et al. (1996). They identify an inverse P Cygni feature which they say could be caused by “structured gas flow onto the white dwarf”, and also conclude that their best fitting model “indicates that the inner edge of the disc may be detached from the white dwarf surface”.

The existence of long-lived accretion belts impacts on predictions of the temperature and flux from the boundary layer (BL) between accretion disc and primary. The standard approach (Pringle & Savonije 1979) gives a BL effective temperature in the range $2 - 5 \times 10^5 \text{ K}$ for high \dot{M} systems, but observations of X-ray fluxes and the ionization of CV winds constrain the BL temperature to $5 - 10 \times 10^4 \text{ K}$ (Hoare & Drew 1991). Accretion onto a non-rotating primary should cause the accretion luminosity released in the disc and in the BL to be approximately equal, but the X-ray flux measured in VW Hyi during outburst shows that the BL luminosity is only ~ 4 percent of that of the disc (Mauche et al. 1991); this is consistent with the low BL temperature deduced from CV winds. Evidently the kinetic energy in the accreting gas is not thermalised and radiated at an equilibrium rate, as assumed in the standard model, but is stored and lost (inwards to the white dwarf and outwards as radiation) over the spin-down lifetime of the accretion belt. This is a consequence of the Low Inertia Magnetic Accretor (LIMA), but the quantitative effect will differ from star to

star depending on the physics of the spin-down (e.g. the intrinsic magnetic field of the primary, the field generated by dynamo action in the belt, the total mass accreted during outburst).

It is useful to keep in mind the energetics of a VW Hyi outburst. Pringle et al. (1987) find that $2.0 \times 10^{-3} \text{ erg cm}^{-2}$ is received over the range $912 - 8000 \text{ \AA}$ during a normal outburst, which is $1.0 \times 10^{39} \text{ erg}$ for a distance of 65 pc (Warner 1987). If this is due to a mass $M(b)$ accreting on to the primary, with half the available potential energy radiated and the other half stored in a rotating equatorial belt, then $G M(1) M(b)/2 R(1) = 1.0 \times 10^{39} \text{ erg}$, which gives $M(b) = 2.2 \times 10^{22} \text{ g}$ for a primary of mass $M(1) = 0.6 M_{\odot}$ (this is compatible with the $\log g = 8.0$ found by Sion et al. (1996)). If 10% of the remaining potential energy is lost in a wind and the rest is stored in an equatorial belt of mass $M(b)$ and angular velocity $\Omega(b)$, then $\frac{1}{2} M(b) R^2(1) \Omega^2(b) \simeq 0.9 \times 10^{39} \text{ erg}$, which gives $\Omega(b) \simeq 0.33 \text{ rad s}^{-1}$, or a rotation period for the belt of $P(b) \simeq 20 \text{ s}$. For a superoutburst, for which the observed radiated energy is 8.4 times larger (Pringle et al. 1987), the accreted mass should be similarly larger.

The predominantly sinusoidal character of DNOs arises from two causes. Petterson (1980) showed that reprocessing from a disc surface in general leads to sinusoidal pulses, independent of inclination. His analysis of the DNO phase shifts that occur during eclipse of UX UMa implies a considerable additional contribution from near the surface of the primary (confirmed in the UV by HST observations: Knigge et al. 1998a). DNOs observed in HT Cas during its outbursts (Patterson 1981) point to the same conclusion. The sinusoidality of this ‘direct’ component from the primary is understandable if the accretion zones are long arcs (perhaps 180° or more in length) running round the equatorial belt, as expected from accretion from the inner edge of a disc.

2.1 Period Discontinuities

In the LIMA the sudden changes in period of the DNOs are attributed to reconnection events (Warner 1995b). Field lines connecting the equatorial belt to an annulus of the accretion disc having angular velocity $\Omega_k \neq \Omega(b)$ will be wound up. Livio & Pringle (1992) suggest that the twist of the field is relieved by reconnection taking place in the magnetosphere of the primary, rather than in movement of the footpoints of the field in the disc or stellar interior. Lamb et al. (1983) find that reconnection will take place after approximately one turn has taken place between the magnetic star and the anchored field (this corresponds to a pitch angle $\gamma \sim 1$ where the field is anchored). Thus a rotation of the primary (or equatorial belt) relative to the disc connection annulus by about 2π radians will break the field lines. State-of-the-art 2D modelling, extrapolated to 3D reality, arrives at the conclusion that “reconnection, leading to periodic (or quasiperiodic) evolution, would be the realistic outcome of the field twisting process” (Uzdensky, Konigl & Litwin 2001).

As pointed out earlier (Warner 1995b), there are no detectable brightness changes at the times of the period jumps. In VW Hyi, which has $L \sim 0.1 L_{\odot}$ towards the end of outburst, we can set any luminosity events as having $\Delta L \lesssim 0.01 L_{\odot}$. A typical observed ‘discontinuity’ is a change

$\Delta\Omega \sim 5 \times 10^{-4}$ within a time $\Delta T \lesssim 100$ s. If a mass $\Delta M(b)$ in the equatorial belt were changing its angular velocity Ω by this amount, the change in rotational energy would be $\Delta E \sim \Delta M R(1)^2 \Omega \Delta\Omega / \Delta T$, which gives $\Delta M(b) \leq 4 \times 10^{14}$ g. It is clear, therefore, that the equatorial belt as a whole is not varying its $\Omega(b)$ in a jerky fashion. We suggest that there are latitudinal variations of $\Omega(b)$, decreasing with increasing latitude towards $\Omega(1)$ of the underlying primary. Reconnection will then produce accretion curtains feeding gas to a range of angular velocities, distributed around the mean value $\Omega(b)$ of the belt. The O - C diagrams of DNOs in TY PsA (Warner, O'Donoghue & Wargau 1989) and in SS Cyg (Cordova et al. 1980) and our observations of VW Hyi (Paper I) do indeed show that the jumps of P can occur in both directions relative to the underlying steady change.

The discontinuities in P , and the lack of any associated luminosity events, constitute probably the most severe constraint on any physical model of DNOs. An attraction of the LIMA model is its ability to feed gas almost effortlessly onto different field lines and hence produce small changes in P .

The inner radius r_0 of the accretion disc is determined by a combination of \dot{M} and field strength (see below). The value of \dot{M} rises and falls during a dwarf nova outburst, decreasing and then increasing r_0 . If $\Omega(b)$ remained at the value determined by its connections to the innermost disc annulus, it (and hence the DNO period) would increase and decrease smoothly as \dot{M} changed. However, the field winding and reconnection process will produce discontinuities. If we suppose that at reconnection the field lines from the primary will reconnect to the innermost disc annulus (at r_0), this being where the field is the strongest, then the change of r_0 and the concomitant change in rotation period $P(b) = 2\pi/\Omega(b)$ will result in reconnection after a time T_R found from $P(b) = \frac{1}{2} \frac{1}{P(b)} \frac{dP(b)}{dt} T_R^2$, or

$$T_R = \frac{\sqrt{2}P(b)}{\dot{P}(b)^{1/2}}. \quad (1)$$

As a quantitative example we may use the observations of TY PsA (Warner, O'Donoghue & Wargau 1989). The DNOs were monoperiodic and increased in period P from 25.2 s to 26.6 s over the first two nights, i.e., $\dot{P} = 1.6 \times 10^{-5}$. There were clear discontinuities of P every $\sim 10^4$ s. Equation 1 gives $T_R \simeq 9 \times 10^3$ s, which is of the correct order of magnitude.

Furthermore, equation 1 provides some qualitative explanation for the observed change of coherence of DNOs during the course of an outburst. Near maximum of outburst \dot{M} is most stable, so $\dot{P} \rightarrow 0$ and the time between reconnections becomes very long. At the end of outburst, \dot{M} is decreasing rapidly and T_R is reduced greatly, leading to frequent reconnections and a DNO signal of low coherence.

Equation 1 can be rewritten as

$$\Delta P \simeq 2P^2(b)/T_R \quad (2)$$

where ΔP is the sudden change in DNO period after a time T_R . This equation is compatible with the limited amount of observational material on DNOs. Its statistical properties could afford a means of testing the LIMA model.

2.2 The Deceleration Phase

The rapid deceleration of the equatorial belt seen at the end of outbursts (Figure 8 of Paper I) has energy and angular momentum implications that limit possible mechanisms. If the deceleration were due to internal viscosity, coupling the belt to the primary, the energy expenditure within or at the base of the belt would be $\dot{E} \sim -M(b) R^2(1) \Omega(b) \dot{\Omega}(b) \sim 3 L_\odot$ for normal outbursts and $\sim 30 L_\odot$ for superoutbursts. This energy loss occurs at a time when the total radiant energy from VW Hyi is only $\sim 0.1 L_\odot$ and the energy radiated by the equatorial belt itself, at $T \sim 3 \times 10^4$ K, is $\sim 0.01 L_\odot$. It would appear more probable, therefore, that the deceleration is a result of magnetic coupling to matter in the disc. We conclude below that the belt energy is transferred to kinetic motion of gas in the disc.

2.2.1 Coupling of the Equatorial Belt and Disc

We look first at angular momentum transfer between the belt and the disc. If the magnetic field is largely generated within the equatorial belt, which itself would rotate nearly as a solid body through the internal magnetic viscosity, but is weakly coupled to the primary, then a simple modification is required to the standard IP model (e.g. Ghosh & Lamb 1979; see also Warner (1995a), Chapter 7, whose notation is adopted here). The rate of change of $\Omega(b)$ is

$$\dot{\Omega}(b) = \frac{n(\omega_s) N_0}{M(b) R^2(1)} \quad (3)$$

where N_0 is the material torque at radius r_0 in the disc, i.e. $N_0 = \dot{M} [G M(1) r_0]^{\frac{1}{2}}$, and $n(\omega_s)$ is the torque function which includes both material and magnetic stresses. ω_s is the “fastness parameter”, given by $r_0 = \omega_s^{\frac{2}{3}} r_{co}$, and r_{co} is the corotation radius in the disc, given by

$$r_{co}^3 = \frac{G M(1)}{\Omega^2(b)}. \quad (4)$$

Using $R_9(1) = 0.73 M_1^{-\frac{1}{3}}(1)$ for the mass-radius relationship of a white dwarf in the range of $0.4 \leq M_1(1) \leq 0.7$, we have

$$\dot{\Omega}(b) = 3.09 \times 10^{-7} n(\omega_s) \omega_s^{\frac{1}{3}} \dot{M}_{16} M_{22}^{-1}(b) M_1^{\frac{4}{3}}(1) \Omega^{-\frac{1}{3}}(b) \quad (5)$$

Typically $n(\omega_s) \sim 0.5$, but it becomes zero when spin equilibrium is reached at $\omega_s = \omega_c \simeq 0.975$ (Wang 1996).

First we consider any dwarf nova during outburst for which the magnetic field generated in the equatorial belt is strong enough to control accretion flow near the primary. For dipole geometry, this condition ($r_0 > R(1)$) gives a field strength $B(b) > 1.5 \times 10^4 M_1^{\frac{2}{3}}(1) \dot{M}_{16}^{\frac{1}{2}} \text{ G}$ (Warner 1995a, equation 7.4b), but in the vicinity of the surface of the primary other higher, and less compressible, multipole components of the field geometry may exist. Suppose that the equatorial belt differs in rotation period by 1 s from its equilibrium period (at which magnetic and material torques balance). Taking $M_{16} = 50$, $\Omega(b) = 0.4 \text{ rad s}^{-1}$ and $M_{22}(b) = 2$, we have $\dot{\Omega}(b) \sim 2.5 \times 10^{-6} \text{ rad s}^{-2}$ from equation 5. The time scale for establishing equilibrium $\tau_{eq} = \Delta\Omega(b)/\dot{\Omega}(b)$ is then ~ 3 h. Therefore, when \dot{M} is high during outburst, the rotation period of the equatorial belt does not differ greatly from its equilibrium value (cf. Popham 1999).

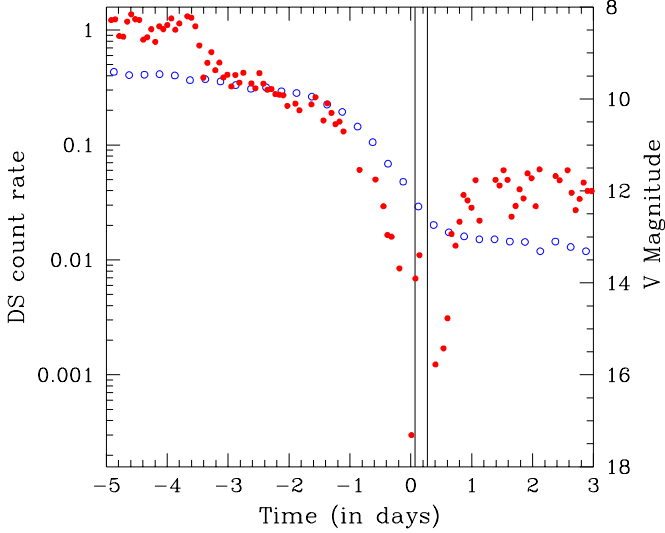


Figure 1. Comparison of EUV flux (filled circles) at the end of a superoutburst with the average optical light curve (open circles). The vertical lines show the range over which the DNOs in Figure 3 of Paper I were observed.

At the end of a VW Hyi superoutburst, however, when $M_{22}(b) \sim 10$ and $\dot{M}_{16} \sim 1$ (as in quiescence), $\tau_{eq} \sim 30$ d and the rapid spin-down cannot be the result of the usual disc torques. A sufficiently powerful torque mechanism exists, however, if the rapid rotation of the belt is able to prevent most accretion by centrifugal action. Such a “propeller mechanism” is thought to act in AE Aquarii, which has a white dwarf rotating with period 33 s and $\dot{\Omega} = -3.9 \times 10^{-16}$ rad s $^{-2}$ (de Jager et al. 1994), giving a spin-down time $\tau \sim 1.7 \times 10^7$ y. If a mechanism of similar power is at work during the rapid spin-down of VW Hyi, we could expect $\tau_{eq} \sim \tau M(b)/M(1) \sim 10$ h, which is similar to what is observed. The inferred energy dissipation in AE Aqr, $I \Omega \dot{\Omega} \simeq 4 L_{\odot}$, is similar to what we deduce for VW Hyi and, as for VW Hyi, is not detected as radiant energy.

In AE Aqr, modelling gives a primary magnetic field of $\sim 1 \times 10^5$ G and a mass transfer rate $\sim 1 \times 10^{17}$ g s $^{-1}$ (Wynn, King & Horne 1997). Accretion onto the primary, found from X-ray emission, is only $\sim 2 \times 10^{14}$ g s $^{-1}$ (Choi, Dotani & Agrawal 1999), which is sufficient to produce accretion regions on the primary and result in modulated X-ray and optical flux (Eracleous et al. 1994). If the VW Hyi rapid spin-down is a propeller stage, we might expect to find a similarly low \dot{M} onto the primary during that phase. This is in fact the case, as we see below from the behaviour of the EUV flux.

It is not surprising that the system gets itself into a propeller phase: at the end of outburst \dot{M} falls rapidly, and so r_0 is increased, pushing the inner edge of the disc towards r_{co} . The spin of the equatorial belt only responds slowly at first to the deceleration torque from the disc, making it easy for r_0 to equal and slightly exceed r_{co} . At this point $\omega_s > 1$ and propeller is inevitable.

2.2.2 EUV Flux as Evidence of Propeller

It is fortunate that there are observations of the EUV flux of VW Hyi that cover the part of the light curve in which we find the rapidly decelerating DNOs. In Fig. 1 we compare the EUV flux during a superoutburst of VW Hyi with the mean optical light curve (the phasing of the two light curves has been achieved using AAVSO and RASNZ data obtained contemporaneously with the EUV observation). The EUV fluxes were measured with the EUVE satellite and have been kindly communicated to us by Christopher Mauche (Mauche, Mattei & Bateson 2001). Whereas the decline phase of the optical light curve is roughly followed by the EUV flux from $V \sim 10$ to $V \sim 11$, there is a steepening of the EUV decline, producing a precipitous fall at $V \simeq 12.2$ and steep recovery starting at $V \simeq 13.0$ (this corresponds to the time of appearance of hard X-rays, mentioned in Paper I (Wheatley et al. 1996)). This is precisely the range during which we see lengthening DNOs and QPOs. The EUV behaviour shows that \dot{M} onto the primary is one or even two orders of magnitude lower at this stage than during quiescence.

During a normal outburst of VW Hyi the EUV flux falls even more steeply than in the superoutburst, taking only ~ 12 h to fall from $\log DS(\text{count rate}) = -1.0$ (when $V \simeq 11.0$) to $\log DS = -2.3$ (Mauche, Mattei & Bateson 2001). The hard (1.5 – 10 keV) X-ray flux at the end of a normal outburst of VW Hyi similarly drops to about zero when V reaches ~ 12.5 (Hartmann et al. 1999).

2.2.3 Spin-down as the Result of Propeller

The nature of the rapid spin-down, if due to propeller, can be explored in the following way. The angular momentum drained from the equatorial belt goes into gas released at the Alfvén radius R_A . For a dipole field geometry, and gas expelled in an equatorial direction, above and below the accretion disc,

$$\frac{2}{3} \dot{M}(\text{wind}) \Omega(b) R(1) R_A \simeq M(b) R^2(1) \dot{\Omega}(b) \quad (6)$$

(Kawaler 1988), which gives, for the $\dot{\Omega}(b)/\Omega(b)$ observed in the February 2000 outburst of VW Hyi,

$$\frac{R_A}{R(1)} \simeq 2.5 M_{22}(b) \dot{M}_{17}^{-1}(\text{wind}). \quad (7)$$

It therefore requires only that most of the gas accreting from the disc be centrifuged out along the rapidly rotating field lines to a few white dwarf radii for a large $\dot{\Omega}(b)$ to result (this gas will not necessarily be ejected from the system as a circumstellar wind; it will rejoin the disc at larger radii (Spruit & Taam 1993)). This is where the $\sim 3 L_{\odot}$ extracted from the belt is hidden: it is in kinetic energy of the centrifuged gas and is not radiated (the same condition applies in AE Aqr). As $\Omega(b)$ is reduced, the field $B(b)$ generated in the belt will drop, which will reduce R_A and terminate the process at some critical $\Omega_c(b)$. In VW Hyi we have not directly observed this transition (our two observational opportunities, on 25 Dec 1972 and 5 Feb 2000, having been terminated by natural causes), but in the outburst of February 2000 DNOs with a period of 40.5 s were observed at the end of our run, so $\Omega_c(b) \leq 0.155$ rad s $^{-1}$ for a normal outburst.

As $B(b)$ is probably larger for a superoutburst, making R_A larger, the propeller should be then more efficient.

It may not be necessary to think of the rapid spin-down phase as a full-blown propeller in action. Spruit & Taam (1993) point out that for the case where the fastness parameter ω_s exceeds unity by only a small amount, mass piles up in the disc and the resulting increase in pressure gradient across the magnetospheric boundary can allow some mass flow across the centrifugal barrier (oscillation about an equilibrium flow eventually is established, but here we are only considering a temporary partial damming up of the flow through the disc). The angular momentum conveyed from the primary to this stored mass is transferred outwards through the accretion disc.

At the end of the rapid spin-down, we see in Figure 8 of Paper I that there is either frequency doubling (as might occur if accretion changed from a single to a two-pole structure) or some spin-up of the equatorial belt. This phase, which occurs at $13.0 \lesssim V \lesssim 13.3$, corresponds to the rapid rise in EUV flux seen in Fig. 1, and also to the second observation during a normal outburst of VW Hyi by the Beppo SAX satellite in the paper by Hartmann et al. (1999), where hard X-rays, which had decreased to about zero during the propeller phase, reappear at $L_x \simeq 9 \times 10^{30}$ erg s⁻¹ and then decay to nearly a factor of two lower in quiescence. A similar, longer term, effect is seen in the EUV after a superoutburst (Fig. 1) where the flux remains higher ($\log DS$ (count rate) ~ -1.3) than the quiescent flux (~ -2.0) for some days (Mauche, Mattei & Bateson 2001). This latter phase corresponds to the brighter V magnitude after superoutburst than after normal outburst (Figure 5 of Paper I).

We suggest that such a spin-up could be expected to follow the propeller phase, because mass that was stored in the inner disc, is eventually allowed to continue accreting on to the primary. This phase accounts for the period of enhanced \dot{M} and should last longer after a superoutburst because the propelling was more powerful and expelled more gas.

By the end of these spin-down and spin-up phases, the effect of the belt's magnetic field on the inner disc will drain the latter in a short time (Livio & Pringle 1992). Rapid rotation of the belt may then continue at an angular velocity sufficient to prevent accretion in the equatorial plane. This can be seen from the estimate that $\dot{M}(1)$ onto the primary during quiescent is found from the hard X-rays to be $\sim 2.5 \times 10^{14}$ g s⁻¹ (van der Woerd & Heise 1987; Hartmann et al. 1999), which is in accord (a) with the requirement that $\dot{M}(1) \ll |\dot{M}(2)|$ in quiescence of a dwarf nova (which stores mass in its disc between outbursts), and (b) with the estimate that the mass transfer rate $\dot{M}(2)$ from the secondary should be about twice that observed in Z Cha (which has outbursts at half the frequency of those in VW Hyi) which is 2×10^{15} g s⁻¹ (Wood et al. 1986).

The radius r_μ of the magnetosphere in an intermediate polar (see, e.g., Warner 1995a) is

$$\begin{aligned} r_\mu &\simeq 1.38 \times 10^{10} \mu_{32}^{\frac{4}{7}} \dot{M}_{14}^{-\frac{2}{7}} M_1^{-\frac{1}{7}}(1) \text{ cm} \\ &= 13 \mu_{32}^{\frac{4}{7}} R(1) \quad \text{for } \dot{M}_{14} = 2.5 \text{ and } M_1(1) = 0.60 \end{aligned} \quad (8)$$

where μ is the magnetic moment, and the corotation radius is

$$r_{co} = 1.50 \times 10^8 P^{\frac{2}{3}} M_1^{\frac{1}{3}}(1) \text{ cm} \quad (9)$$

and therefore $r_\mu > r_{co}$ unless $\mu_{32} \leq 2.8 \times 10^{-2}$, or $B(1) \leq 4.5 \times 10^3$ G (this may be compared with the conditions at the peak of outburst, where $\dot{M}(1) \sim 5 \times 10^{17}$ g s⁻¹ and the requirement that $r_\mu > R(1)$ in order to produce the magnetically channelled accretion implied by the 14 s modulation gives $B(1) > 7.7 \times 10^4$ G). Therefore, it would need an extremely weak field to allow the magnetosphere in quiescence to be compressed to the point where accretion as an IP is allowed. The small amount of accretion that manages to reach the primary is evidently not predominantly magnetically channelled (from the absence of DNOs in the optical or in the hard X-ray flux: Belloni et al. (1991) – these authors only examined the region 13–15 s, looking for X-ray modulations similar to those seen at maximum of outburst. A more catholic search in the various hard X-ray light curves, for periods in the range of 20–100 s, should be made.), and may be a result of more isotropic accretion from a hot corona, as in the models of van der Woerd & Heise (1987) and Narayan & Popham (1993), which extends to a distance $\sim R(1)$ above the surface of the primary when the gas becomes optically thin in the X-ray region.

2.2.4 The Post-outburst Equatorial Belt

The detection in VW Hyi (Sion et al. 1996) of rapidly rotating equatorial belts one day after a normal outburst (and covering ~ 11 percent of the surface area of the primary) and 10 days after a superoutburst (covering reduced to ~ 3 percent) shows that although the belt may persist throughout the average ~ 28 d of quiescence, its spin-down time scale is comparable to the outburst interval. Therefore the torques acting during outbursts are largely on the gas accreted during the outburst, with little allowance required for gas left from the previous outburst.

The hot belt left at the end of outburst contains the thermal energy of compression and kinetic energy of rotation which will partly be thermalised internally by viscous stresses and partly lost by magnetic coupling to the disc. Even if there is no magnetically controlled accretion during quiescence, coupling still exists through field lines connecting the belt to the slower rotating parts of the accretion disc, and through possible continued weak propelling. The thermal energy in the belt is partly radiated (as seen by its temperature excess over the ~ 18000 K quiescent temperature of the primary) and partly conveyed into the primary. The latter is detected through the excess temperatures of the primary measured by Sion et al.

The observed $v \sin i$ for the primary of VW Hyi is 300 km s⁻¹ (Sion et al. 1996) which, with $i \sim 60^\circ$, gives a rotation period of the primary of $P(1) \simeq 157$ s. The kinetic energy in the belt at the end of the propeller phase is $\frac{1}{2} \dot{M}(b) R^2(1) \{\Omega(b) - \Omega(1)\}^2$, which is $\sim 5 \times 10^{38}$ erg if $P(b) \sim 40$ s and $M_{22}(b) \sim 5$. All of this must be lost in ~ 25 d (in order to maintain a steady state), requiring an average luminosity of $0.06 L_\odot$, or 4.5 times the luminosity of the steady state 18000 K primary (Long et al. 1996). This energy loss is readily accounted for by the observed cooling of the belt and primary. Some of the energy will of course be transferred to the interior through viscous coupling of the belt to the interior. In VW Hyi this coupling is evidently

quite weak, possibly implying a relatively weak magnetic field in the primary – which is slightly ironic in view of the fact that VW Hya supplies so many observable magnetically related phenomena at the end of its outbursts.

2.3 Magnetic Modelling

Here we will give a few plausibility arguments for the LIMA model.

2.3.1 Transmission of Accretion Stress to the Interior

To couple the exterior of a star to its interior requires a process that can transfer stresses. A non-magnetic, non-crystalline core of a white dwarf requires $\gtrsim 5 \times 10^{10}$ y to transport angular momentum (Durisen 1973), but the high stability of the rotation of DQ Her shows that magnetic accretors are able to couple surface torque to the deep interior. As pointed out by Katz (1975), following the early work of Mestel (1953), a relatively small magnetic field is able to provide the means of coupling. This can be seen as follows.

The stress $Rd(\rho v)/dt$ of accretion can be transported to the interior by the Maxwell stress of field lines, if $B^2/4\pi$ is considerably larger than the mechanical stress. That is,

$$B^2 \gg 4\pi\rho\dot{\Omega}R^2(1) \quad (10)$$

or

$$B \gg 14\rho^{\frac{1}{2}}\dot{M}_{17}^{\frac{1}{2}}M_1^{-\frac{5}{8}}(1) \text{ G} \quad (11)$$

where we have made similar approximations to those used in earlier Sections.

Quite small fields are therefore capable of stiffening the outer regions of white dwarfs (in particular, causing almost solid body rotation in an equatorial belt), but for $\rho \simeq 10^6 \text{ g cm}^{-3}$, which in an intermediate mass white dwarf occurs at a depth where $\sim 20\%$ of the mass has been traversed, it requires $B \gg 2 \times 10^4 \text{ G}$ to couple to the rest of the interior. Fields $\gtrsim 10^5 \text{ G}$ therefore are required to transport angular momentum throughout the star[‡].

2.3.2 Field Enhancement by the Equatorial Belt

An estimate of the enhancement of the intrinsic field of the primary caused by accretion around the equator may be obtained as follows. The radial component $B_r(1)$ of the primary is converted into toroidal field $B_\phi(b)$ of the belt as the field lines are carried around by the conducting fluid flow. In one rotation of the belt, a field strength $B_\phi(b) \simeq B_r(1)$ is generated (e.g., Livio & Pringle 1992) and this increases proportional to the accumulative angle (we assume here that $\Omega(b) \gg \Omega(1)$). Magnetic flux is lost on a time scale τ , and hence the mean field strength is

$$B_\phi(b) \simeq B_r(1) \frac{\tau}{P(b)}. \quad (12)$$

[‡] Note that the exceptional spin-down power of AE Aqr (de Jager et al. 1994) is based on the assumption that the primary rotates as a solid body. The field strength $B \sim 1 \times 10^5 \text{ G}$ deduced by Choi and Yi (2000) would suggest that this is not necessarily the case: it is possible that only the outer parts are being spun down.

Table 1. Field strengths in the equatorial belt

$B_r(1)$	10^3 G	10^4 G	10^5 G
$B_\phi(b)$	$1.2 \times 10^4 \text{ G}$	$3.8 \times 10^4 \text{ G}$	$1.2 \times 10^5 \text{ G}$

If the loss mechanism is bouyancy of the field, rising at the Alfvén velocity v_A , then $\tau \simeq H/v_A$, where H is the scale height and $v_A = B_\phi(b) (4\pi\rho)^{-\frac{1}{2}}$, which gives

$$B_\phi^2(b) \simeq \frac{\Omega(b)H}{\pi^{\frac{1}{2}}} \rho^{\frac{1}{2}} B_r(1). \quad (13)$$

Using $\rho H = M(b)/2\pi x R^2(1)$, where $xR(1)$ is the (latitudinal) width of the accretion belt, and an effective gravity of $g_{eff} = yg$, where $g = GM(1)/R^2(1)$, we find

$$B_\phi(b) \simeq 210 B_r^{\frac{1}{2}}(1) P^{-\frac{1}{2}}(b) \left(\frac{M_{22}(b)T_5}{xyM_1(1)} \right)^{\frac{1}{4}} \text{ G} \quad (14)$$

where $B_\phi(b)$ and B_r are measured in Gauss, $P(b)$ in secs and T_5 is the temperature in the belt in units of 10^5 K .

Using $x = 0.1$, $y = 0.01$ (as indicated by $\log g = 6.0$, found by Sion et al. 1996), we have, for $P = 20 \text{ s}$, $M_{22}(b) = 4$, the field strengths as given in Table 1, and therefore some field enhancement appears feasible. The geometry of a rotation-enhanced field is probably quite complicated. The B_ϕ component estimated here will determine the radius of the inner edge of the accretion disc, and any region with a strong radial component will allow accretion onto the primary. This same radial field is responsible for propelling.

2.3.3 Predicted and Observed P - \dot{M} Relationships

Magnetically channelled accretion flow at the inner edge of the accretion disc requires that the magnetospheric radius of the primary be larger than the stellar radius. This condition may be written (e.g. equation 7.4b of Warner 1995a)

$$B(b) \gtrsim 4.7 \times 10^4 M_1^{\frac{2}{3}}(1) \dot{M}_{17}^{\frac{1}{2}} \text{ G} \quad \text{for a dipole field} \quad (15)$$

$$B(b) \gtrsim 9.0 \times 10^3 M_1^{\frac{2}{3}}(1) \dot{M}_{17}^{\frac{1}{2}} \text{ G} \quad \text{for a quadrupole field} \quad (16)$$

For accretion from as close to the primary as in dwarf novae in outburst, any quadrupole component of the field geometry is therefore likely to dominate (see also Lamb 1988). Comparison of Table 1 and equations 15 and 16, indicates that magnetically controlled accretion into the equatorial belt is plausible even for intrinsic fields $B_r(1)$ as small as 10^3 G .

In the LIMA model the predicted DNO periods are

$$P \propto \mu^{\frac{6}{7}} \dot{M}^{-\frac{3}{7}} \quad \text{dipole} \quad (17)$$

$$P \propto \mu^{\frac{6}{11}} \dot{M}^{-\frac{3}{11}} \quad \text{quadrupole} \quad (18)$$

(Warner 1995b). Mauche (1997) has shown that in SS Cyg, the DNO periods behave more as $P \propto \dot{M}^{-\frac{1}{10}}$ (where \dot{M} is obtained from the EUV flux). This weak dependence on \dot{M} is readily understandable with the LIMA model.

First we note that, with $M(b)$ held constant, equations 14, 17, 18 predict (since $\mu \propto B \propto P^{-\frac{1}{2}}$ in equation 14) $P \propto \dot{M}^{-\frac{3}{10}}$ for dipole and $P \propto \dot{M}^{-\frac{3}{14}}$ for quadrupole. But $M(b)$ increases during an outburst, as $M(b) = \int_0^t \dot{M} dt$, and this in equation 14 enhances $B_\phi(b)$ which acts to decrease

further the dependence of P on \dot{M} . It is, for example, possible to obtain $P \propto \dot{M}^{-\frac{1}{10}}$ by allowing $\log \dot{M}$ to vary approximately parabolically with time, as in the models of SS Cyg computed by Cannizzo (1993).

3 THE QUASI-PERIODIC OSCILLATIONS

In this section we explore the suggestion that the QPOs are the result of vertical oscillations of selected annuli of the accretion disc. As already outlined in Section 3 of Paper I, the reason for considering such oscillations is that they can provide luminosity modulations at periods much longer than those of the DNOs.

3.1 Location of the QPOs

The systematic study of wave propagation in accretion discs given by Lubow & Pringle (1993; hereafter LP) and the numerical results given by Carroll et al (1985) show that QPOs with periods greater than about 100 s arise from nonaxisymmetric modes. In particular, it is the $m = 1$ prograde (i.e., moving in the same direction as Keplerian motion, as viewed from an inertial frame) modes which can be excited. These modes are equivalent to a vertical thickening of the disc over an extended range of azimuth which travels retrogradely in the frame of rotation of the disc, but at a slightly lower angular frequency than that of the Keplerian rotation. Figure 12c of LP shows that low frequency retrograde waves are unable to propagate (in LP's notation, $K_x^2 < 0$ for small F) but low frequency prograde modes waves can propagate ($K_x^2 > 0$ for small F in Figure 12b). LP's final conclusion is that "the $m = 1$ g-mode appears to provide the best propagational properties near the disc centre".

To generate oscillations an excitation mechanism is required, which must be selective in order to produce the distinctive time scales seen in individual CVs. There are three radii within an accretion disc in which excitation mechanisms might arise: (a) the annulus in the disc at which any stream overflow impacts onto the disc, (b) the inner edge of the disc, near radius r_0 , and (c) the outer edge of the disc where stream impact occurs.

The stream overflow impact on the inner disc occurs close to the stream's radius r_{min} of closest approach to the primary (Lubow & Shu 1975; Lubow 1989) which, as a fraction of the separation of the centres of mass of the stellar components, is at

$$\frac{r_{min}}{a} = 0.0488q^{-0.464} \quad (19)$$

(Warner 1995a) where q is the mass ratio (secondary mass $M(2)$ divided by primary mass $M(1)$). The Keplerian velocity is

$$v_k(r) = \left(\frac{GM(1)}{r} \right)^{\frac{1}{2}} \quad (20)$$

from which, with Kepler's Third Law, we obtain the Keplerian period as a fraction of the orbital period:

$$P_k(r_{min})/P_{orb} = 0.0107q^{-0.70}(1+q)^{\frac{1}{2}}. \quad (21)$$

For a star such as VW Hyi, with $q \simeq 0.15$ and $P_{orb} \simeq$

100 min, we have $P_k(r_{min}) \sim 300$ s. It is therefore conceivable that QPOs with periods of hundreds of seconds could be excited by the stream overflow process.

Our observations of VW Hyi in February 2000, however, show that there is an evolution of QPO period which parallels that of the DNOs, and these are different from those observed in December 1972. QPOs excited by stream impact would be expected to have a fixed time scale. Furthermore, stream impact (which occurs at a greater velocity than the local Keplerian velocity) is unlikely to excite waves that are retrograde in the Keplerian rotating frame (as appears to be required by some of our observations).

Although some of the QPO periods in CVs are comparable to the Keplerian period at the outer edge of the disc, and might be oscillations excited by the initial stream impact (at the bright spot), the periods of 250 – 500 s seen in VW Hyi are too short ($P_k/P_{orb} \sim 0.2$ at the outer edge of the disc (equation 8.6 of Warner 1995a) which is ~ 1300 s for VW Hyi), and the evolution towards longer periods seen at the end of outburst occurs at a phase when the outer radius of the disc is known to be shrinking (e.g., in Z Cha: O'Donoghue 1986), which would produce decreasing periods.

We therefore turn to consideration of oscillations located near the inner edge of a truncated disc.

3.2 Inner Disc QPOs and their interaction with DNOs

For the low field white dwarfs in dwarf novae the inner edge of the disc is close to the primary, so opportunities for a bulge to intercept radiation from the central source are relatively high. In particular, a travelling wave running around the inner disc will intercept some of the constant luminosity component of the primary, producing (a) modulation as its illuminated surface is seen at different aspects, (b) modulation as it obscures radiation from the central source (as seen by us), and (c) a shadow cast over the illuminated concave surface of the accretion disc. Interruption and obscuration will also affect the rotating beam which is the source of the DNOs. The relative importance of these effects will depend partly on orbital inclination - e.g., they will have a maximum effect at high inclination. At low inclination all but one of the effects should disappear: there is still the possibility of a travelling bulge intercepting the rotating beam and generating optical DNOs (which will be at a lower frequency than any simultaneous X-ray DNOs, see below). The contributions of these several components are likely to vary rapidly with time, as the amplitude and profile of the travelling bulge changes. This accounts for the wide range of behaviour in the interactions between the DNOs and QPOs described in Section 4.2.3 (and Figures 20 and 21) of Paper I.

3.2.1 Production of QPOs by a Travelling Wave

We consider the interception of radiation from the primary by a vertical thickening of the disc caused by a travelling wave. To produce an amplitude Δm in the light curve requires a wave of height $h \sim \pi \Delta m r_0$ if the wave has a sinusoidal profile, radiation is emitted uniformly over the surface

of the primary, reprocessing is highly efficient, and we see all of the wall. This last requirement – that the primary does not obscure any of the far side of the wall – translates to $r_0/R(1) \geq (1 - (h/r_0) \tan i)^{-1} \sec i$. Taking $i \simeq 60^\circ$ for VW Hyi we have $r_0/R(1) \geq 2.1$ for $h/r_0 = 0.10$. As we are mostly dealing with QPOs observed during the propelling phase, where the inner edge of the disc is at a few times $R(1)$ (see equation 7) this condition is satisfied for even quite high QPO walls. For higher inclination systems, or for smaller r_0 in VW Hyi, reprocessing from the far side of the wall may be largely obscured by the primary.

The mean amplitude of QPOs seen in Figure 1 of Paper I is $\simeq 0.05$ mag which, from the above, requires $h/r_0 \simeq 0.15$. At this time the primary in VW Hyi has a temperature of at least 25 000 K (Gänsicke & Beuermann 1996), i.e., $L \geq 2.0 \times 10^{32}$ erg s $^{-1}$. The fraction of this, if radiated isotropically, intercepted by the wall is $\sim h/\pi r_0 \sim 1.0 \times 10^{31}$ erg s $^{-1}$. At the end of outburst, VW Hyi has $L \sim 4 \times 10^{32}$ erg s $^{-1}$ in the optical region (Pringle et al. 1987). If reprocessing into the optical is very efficient we would therefore expect an amplitude ~ 0.025 mag. However, in reality most of the radiation comes from the hot equatorial belt, which is both closer to the wall and more luminous than most of the surface of the primary, so QPO amplitudes of 0.05 mag or more are energetically feasible.

The roughly constant amplitude (on a magnitude scale) of the QPOs in Figure 1 of Paper I shows that a constant fraction of the radiation emitted by the central source is being periodically intercepted. It suggests that at this late phase of the VW Hyi outburst the brightness in the optical is largely due to reprocessed radiation from the hot primary, rather than intrinsic luminosity of the accretion disc. This is also seen by the very large amplitude of the QPOs in the 12 Sep 1972 observation (Figure 12 of Paper I), where reprocessing from the travelling wall at times accounts for a large fraction of the system brightness. Note also that at the end of a superoutburst the fall to quiescent magnitude is slower than in normal outbursts (Figure 5 of Paper I). This may be due to the larger decay time of irradiation by the more massive equatorial belt.

Alternate reprocessing and obscuration is particularly marked in the section of the 19 Dec 2000 run shown in Fig. 2. The minima of the QPO modulation clearly pull the system brightness well down below the smoothed average, both on and between the orbital humps. Notice in particular in the upper panel of Figure 12 of Paper I that a large dip between the orbital humps is immediately followed by a large peak – evidently the wall was of exceptional height for that revolution; the central part of the light curve on 6 November 1990 (Figure 12 of Paper I) also shows this, where the obscuring wall survives for several revolutions. Two short lived periodic dips can also be seen in Fig. 2; one around HJD 2451898.5 at a period 342 s for about 3 cycles, and another QPO modulation in the last part of the run at 382 s. In this latter QPO, deep dips are seen at twice the QPO period, i.e. at 760 s, cutting well into the orbital hump (marked by the arrows).

Periodic obscuration of the central source by a travelling bulge should lead to a periodic component in the absorption spectrum. It is possible that in VW Hyi this has already been seen: Huang et al (1996) observed VW Hyi at super-maximum with the HST and found deep narrow absorption

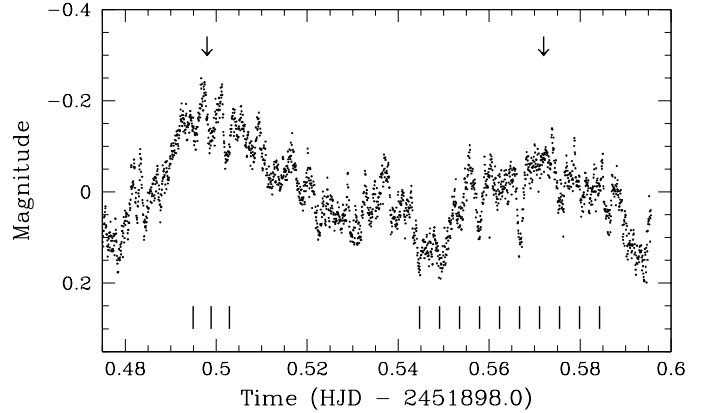


Figure 2. Part of the light curve of VW Hyi obtained on 19 December 2000. Prominent periodic dips are marked by vertical bars. Arrows indicate predicted times of orbital hump maxima.

cores in N V and C IV lines in one spectrum, which had disappeared in a second spectrum taken ten minutes later. A prediction of our model is that such variation in the column density, if caused by the rotating bulge in the inner disc and not by, e.g., absorption by the accretion stream, should be modulated at the QPO period.

3.2.2 Interception of the DNO Beam by the Travelling Wave

Reprocessing of the rotating beam by the travelling bulge generates a second set of DNOs whose frequency is the difference between the beam and bulge frequencies. That is, at a reprocessed period $P_{DNO'} = (1/P_{DNO} - 1/P_{QPO})^{-1}$. This is the relationship we have found in VW Hyi (Figure 18 of Paper I). The waveform of the reprocessed DNOs will be a convolution of the profile of the DNO beam and that of the bulge. If the bulge is non-sinusoidal then the reprocessed profile will have harmonics in it. This is seen in our observations. There is, however, another possibility. Suppose that there are two accretion zones, as in dipolar accretion, with one above the equator and the other (perhaps 180 degrees away in longitude) below the equator. The rotating beam from the former will illuminate the upper surface of the disc, generating optical DNOs observable by us, but the latter illuminates the under surface of the disc which is invisible to us. The travelling bulge, however, may intercept radiation from both accretion zones, reprocessing it to become a modulated optical signal visible to us (when the bulge is at ‘superior conjunction’). This signal will in general show both a fundamental and first harmonic, arising from the different intercepted fluxes of the two rotating sources of illumination.

3.3 Excitation of QPOs

Although eigenmode analyses of complete accretion discs have been made (see Section 3 of Paper I), excitation mechanisms in magnetospherically truncated discs do not appear to have been explored. Here we suggest a possible mechanism, based on the standard IP model, which may excite modes of the correct period and which also seems capable

of explaining why the ratio of DNO to QPO period remains roughly constant during our observations of VW Hyi made in February 2000.

In the model of accretion from a disc into a magnetosphere (Ghosh & Lamb 1979) outlined in Section 2, there are three radii of importance: the largest is the corotation radius r_{co} at which the angular velocity $\Omega(1)$ of the magnetosphere matches the Keplerian velocity; then comes r_0 at which the magnetosphere begins to influence the fluid flow in the disc, where for $\omega_c = 0.975$, $r_0 = 0.975^{\frac{2}{3}} r_{co} = 0.983 r_{co}$ for the equilibrium state; finally there is r_A where the disc flow matches the magnetospheric rotational velocity and accretion along field lines becomes possible. The region contained within $r_A \leq r \leq r_{co}$ is therefore one where the disc flow speed is greater than the speed of the field lines. The field lines consequently are dragged forward by the plasma, producing a spin-up torque on the primary or its equatorial belt. Conversely, we can think of that region (Ghosh and Lamb's 'boundary layer') as one where the torque from the magnetosphere decelerates the accretion flow until it matches the magnetospheric angular velocity. This deceleration zone (DZ) is a plausible site for exciting disc oscillations.

Consider equilibrium accretion (i.e. with \dot{M} constant). In general the primary or its equatorial belt will have an inclined magnetic axis (an aligned, symmetrical field would produce annular accretion zones around each rotation pole and not generate the anisotropic radiation pattern required for observable DNOs). There will be an azimuthal variation of field strength around the DZ. The strongest field lines threading the DZ will occur at a particular azimuth. As the plasma attached to those field lines advances relative to the rotation flows at r_A and r_{co} on either side of it, it drags the field lines forward, is decelerated in the process and piles up and is shocked by gas following in the same annulus threaded by weaker field lines. This heats and thickens the disc in this region. Gas may also be lifted out of the disc in this region as the field lines are bent over by the twisting motion and provide some vertical magnetic pressure support. The result is a region of higher density and greater vertical thickness (a 'blob', to adopt a frequently used technical term).

The growth of the blob terminates when the field lines threading it have advanced so far relative to the $\Omega(1)$ rotation that they break and reconnect to the disc in an energetically more favourable position. The sudden release of the blob from its decelerated and elevated state will provide the perturbation required to launch a travelling wave at a speed determined by the local conditions in the annulus. This wave may damp out quite quickly, but it will be re-generated at the next reconnection event. The time scale of wave generation will then be determined by the recurrence period of reconnections; there is possibility of a resonance which would generate waves of considerable amplitude.

The time scale of reconnection can be estimated as follows. Let the angular velocity of the plasma in the region of strongest field threading be $\Omega(max)$. If reconnection occurs when the field lines have advanced through an angle θ relative to their untwisted position, then the time T_R between reconnections is given by

$$T_R[\Omega(max) - \Omega(1)] = \theta. \quad (22)$$

Typically $\theta \sim 2\pi$ (Lamb et al. 1983), and Ghosh & Lamb (1978) show that the angular frequency $\Omega(r)$ is max-

imum at $r = r_0$, therefore $\Omega(1) < \Omega(max) < \Omega(r_0)$. The value of $\Omega(max)$ appropriate for the present need is not available from existing models of the DZ: in the models given by Ghosh & Lamb, the greatest magnetic dissipation and consequent deceleration occurs close to the inner boundary at r_A , but the details of this model are disputed by Wang (1987).

If we identify T_R as the time scale that will resonate with the disc oscillation, and adopt $\Omega(max) \simeq \Omega(r_0)$, we have

$$\frac{P(QPO)}{P(DNO)} = \frac{\omega_s}{1 - \omega_s}. \quad (23)$$

The observed ratios $P(QPO)/P(DNO)$ are in the range 10 - 20, implying values of ω_s in the range 0.91 - 0.95.

Equation 23 has the property that, for $\omega_s \simeq$ constant, $P(QPO) \propto P(DNO)$, as is seen in VW Hyi in the February 2000 observations.

It may be noted that the winding and reconnection of field lines described here should also occur in the intermediate polars. With typically $P(1) = 15$ minutes, equation 23 shows that any resonant QPO would have a period of \sim few hours, which is comparable to the orbital period and would be difficult to detect photometrically.

In systems of low orbital inclination, luminosity modulation at the revolution period of the travelling wall would not be expected – but the growth and decay of a wall, re-processing radiation into our direction, could lead to QPOs with mean periods equal to the average *lifetime* of the wall.

In some of our light curves, particularly Figure 1 of Paper I, we have the impression that, apart from photon counting and scintillation noise, almost all of the observed rapid variations are due to DNO and QPO modulation – the rapid flickering associated with CVs is weak or absent. If the normal flickering activity is associated with magnetic instabilities in the inner disc (e.g. Bruch 1992), this may indicate that the presence of QPOs, requiring a more organised magnetic structure, suppresses the flaring activity.

Unless there is another, nonmagnetic, excitation mechanism for QPOs, our observations of occasional QPOs during quiescence (Section 4.2.2 of Paper I) shows that some magnetic disc–primary interaction can occur at minimum light, even if little or no magnetically controlled accretion occurs.

4 APPLICATION TO OTHER SYSTEMS

Several of the DNO and QPO phenomena that we observe in VW Hyi are present in other cataclysmic variables. The models that we have developed for VW Hyi throw some light on what is happening in these other systems.

4.1 X-ray and EUV DNOs in SS Cyg

The only DNOs in VW Hyi observed in the X-ray region are those analysed by van der Woerd et al. (1987). Soft X-ray modulation with a period of 14.06 s and mean amplitude of 15% was found towards the end of the plateau ($V = 9.4$) of the November 1983 superoutburst, and oscillations with periods of 14.2 to 14.4 s were found near the peak ($V = 8.8$) of the October 1984 superoutburst. Extensive observations

by EXOSAT of these and other VW Hyi outbursts showed no other instances of DNOs.

On the other hand, DNOs in the X-ray and EUV regions have been extensively observed during SS Cyg outbursts. We will therefore briefly describe the SS Cyg observations and suggest a model to account for them which, *mutatis mutandem*, may also apply to VW Hyi.

4.1.1 DNOs in SS Cyg

Optical DNOs in the period range 7.3 – 10.9 s are observed in SS Cyg during outburst (see references in Warner 1995a), and soft X-ray DNOs are observed in the same range (Jones & Watson 1992 and references therein). Only recently have the two spectral regions been observed simultaneously, establishing the identity of periods (C. Mauche, private communication). DNOs in the EUV region (100 – 200 Å) have been observed in several outbursts of SS Cyg (Mauche 1996a,b, 1997, 1998) with the aid of the EUVE satellite. An advantage of working in the EUV is that the flux directly monitors $\dot{M}(1)$. The long expected $\dot{M}(1) - P$ correlation has been confirmed (the $V - P$ relationship is multivalued because the $V - \dot{M}(1)$ relationship is different on the rising and falling branches of a dwarf nova outburst). The most dramatic observation, however, is the discovery of frequency doubling during the outburst of October 1996 (Mauche 1998), producing DNOs with $P \sim 3$ s. A similar period was observed in X-ray DNOs during the subsequent outburst (van Teeseling 1997). At the maxima of two earlier outbursts (August 1993 and June 1994) the otherwise purely sinusoidal EUV DNOs were found to contain substantial components of first harmonic (Mauche 1997), suggestive of incipient transition to a frequency doubled state.

4.1.2 The Geometry of Accretion by a Weak Field

As a possible explanation of this behaviour we consider the nature of accretion from the inner edge of a truncated disc into the magnetosphere of a primary with a weak magnetic field. For weak fields and large \dot{M} , cooling of an accretion flow is effected by bremsstrahlung radiation. The height h_s of the shock above the surface of the primary is (Lamb & Masters 1979; see equation 6.15 of Warner 1995a)

$$h_s = 9.6 \times 10^7 M_1(1) R_9^{-1}(1) N_{16}(e) \text{ cm} \quad (24)$$

where $N_{16}(e)$ is the electron density (in units of 10^{16} cm^{-3}) in the post-shock region. Using a post-shock velocity $v^2 = GM(1)/8R(1)$, the continuity equation $\rho v/B \propto \rho v r^3 = \text{constant}$ for fluid flow in dipole geometry, and a fractional area of the white dwarf surface covered by the accretion zone $f = 0.25(R(1)/r_0)(\delta/r_0)$, where δ is the width, within the DZ, of the accreting zone of the disc (Wickramasinghe, Wu & Ferrario 1991), we find

$$N(e) = 1.48 \times 10^{14} \left(\frac{r_0}{\delta}\right) \omega_s^{\frac{2}{3}} \dot{M}_{17} R_9^{-\frac{5}{2}}(1) M_1^{-\frac{1}{6}}(1) P_1^{\frac{2}{3}}(1) \left(1 + \frac{h_s}{R(1)}\right)^{-3} \text{ cm}^{-3} \quad (25)$$

where $P_1(1)$ is the spin period of the primary (or equatorial belt) in units of 10 s, and the radius of the inner edge

of the disc (from the discussion in Section 2.2.1) is taken to be

$$r_0 = 6.96 \times 10^8 \omega_s^{\frac{2}{3}} M_1^{\frac{1}{3}}(1) P_1^{\frac{2}{3}}(1) \text{ cm}. \quad (26)$$

The stand-off shock height will be within the field-dominated accretion flow if

$$\frac{h_s}{R(1)} < \frac{r_0}{R(1)} - 1. \quad (27)$$

If, from equations 24, 25 and 26, it emerges that $h_s > r_0 - R(1)$ then there is no shock, and flow from the inner edge of the disc to the primary is pressure supported and subsonic.

Three regimes can be identified:

(i) $h_s > r_0 - R(1)$. This will happen at low $B(1)$ and low \dot{M} (see Figure 1 of Wickramasinghe, Wu & Ferrario 1991) and produces no shock-heated accretion zones (other than the DZ).

(ii) $h_s < r_0 - R(1)$, but $h_s \gtrsim 1.2R(1)$. Here the shock-heated parts of the accretion curtains stand well above the surface of the primary and (depending on orbital inclination) both may be visible to an outside observer – but only one is visible to (and hence irradiates) each surface of the disc.

(iii) $h_s \ll R(1)$. This requires relatively high \dot{M} , as possibly achieved at the maxima of dwarf novae and in nova-like variables. Because of the large cross sectional area of the accretion flow, it may be of low optical thickness along the flow, but optically thick in the transverse direction.

Regimes (ii) and (iii) correspond roughly to the IP structures described by Hellier (1996), Allan, Hellier & Beardmore (1998) and more completely by Norton et al. (1999). These authors show that two-pole disc-fed accretion will lead to a single X-ray pulse per rotation if the transverse optical depth of the accretion flow is low, but along the flow the optical thickness is high (which results in a superposition of the radiation maxima from the two accretion zones), whereas two pulses per cycle arise if the roles of the transverse and longitudinal optical depths are reversed. Among the IPs, the smaller values of $P(1)$ (~ 100 s) are double pulsed and the longer period (~ 1000 s) systems are single pulsed. In the dwarf novae, the combination of (variable) field strengths and \dot{M} variations may be leading to successive passage through the various regimes.

Even without changes in optical depths, regime (iii) introduces geometric complications for primaries with low fields. Equation 26 shows that the inner edge of the disc is close to the surface of the primary. As a result, obscuration of part or all of one hemisphere of the primary, or even of the accretion zones in equatorial regions, can occur. For example, for $r_0 \lesssim 1.2R(1)$, for orbital inclinations that are at least moderate, the primary obscures the accretion zones when they are on its far side, and the disc may obscure them for much of the phases when they are on the near side. This leaves the upper accretion zone visible only on each side of the primary, i.e. twice per rotation, producing a first harmonic dominated light curve.

The observations of DNOs in SS Cyg enable this model to be made partially quantitative. Models of SS Cyg outbursts (Cannizzo 1993) give $\dot{M}(1) \simeq 6 \times 10^{17} \text{ g s}^{-1}$ at maximum luminosity, but the recent HST parallax determination (Harrison et al. 1999) gives a distance about twice that

adopted by Cannizzo, so we increase the latter's \dot{M} value by a factor of four. The EUVE observations show that DNOs first appear, with $P \simeq 9.5$ s, at about 25% of the maximum EUV luminosity, and that frequency doubling occurs (from $P \simeq 5.8$ s to $P \simeq 2.9$ s) when $L \simeq 90\%$ of maximum luminosity. If we identify the turn-on of DNOs as the transition from regime (i) to (ii), then this occurs at $\dot{M}_{17} \simeq 6.0$. SS Cyg has an unusually large $M(1)$ (Robinson, Zhang & Stover 1986) – as indeed it must have in order to allow DNOs as short as 6 s. We take $M(1) = 1.20$, in which case $R_9(1) = 0.385$.

If we treat (δ/r_0) and ω_s as unknowns, then the condition $h_s = r_0 - R(1)$, equations 24, 25, 26, and the parameters for SS Cyg, produce $r_0/R(1) = 1.69$, $\omega_s = 0.87$ and $\delta/r_0 = 0.13$, where we have made use of the additional relationship $\delta/r_0 \simeq (1 - \omega_s)$ (Wickramasinghe, Wu & Ferrario 1991). Too much should not be deduced from these figures – but the fact that a physically sensible solution is found at all is encouraging. Taking a step further, keeping δ/r_0 and ω_s fixed and calculating h_s when $\dot{M}_{17} = 20$ (i.e. when the first harmonic appears), gives $r_0/R(1) \simeq 1.25$ and $h_s/R(1) \simeq 0.02$ which should certainly lead to strong geometric effects and the production of first harmonic effects in the X-ray/EUV region.

We note that the EUV fluxes of SS Cyg and U Gem, at the ends of normal outbursts, also show dips (Mauche, Mattei & Bateson 2001). It will be interesting to see whether DNOs, if present at these times, also have more rapid period increases, indicative of propelling.

4.1.3 DNOs in AH Her and VW Hyi

In AH Her DNOs are present on the rising branch of outburst, disappear about 0.5 d before optical maximum and reappear about 2 d after maximum. These phases are probably more symmetrically placed about EUV or \dot{M} maximum. The observations and analyses (Stiening, Hildebrand & Spillar 1979; Hildebrand et al. 1980) are sufficient to show that frequency doubling does not occur, which might otherwise have accounted for the disappearance. For VW Hyi, however, we have occasional glimpses of the evolution of the DNO period down to a minimum of 14.06 s, also with no indication of frequency doubling. The low success rate of detecting DNOs in VW Hyi for $P \lesssim 20$ s suggests that more complete coverage of AH Her could also be successful, and that the observed minimum at $P = 24.0$ s does not represent the period at which the magnetosphere is crushed to the surface of the primary.

The appearance of DNOs at 14.06 ± 0.01 s in two separate outbursts in VW Hyi (Section 4.2.1 of Paper I), and the fact that this is the minimum observed period and that it occurs several days after maximum $\dot{M}(1)$, may mean that magnetically channelled accretion is absent at the highest $\dot{M}(1)$, but a brief and slight reduction allows the establishment of channelled flow. In this case, with the Nauenberg (1972) mass–radius relationship for white dwarfs, and the assumption that 14.06 s is the Kepler period at the surface of the white dwarf, we have $M_1(1) = 0.702$ for VW Hyi. For comparison, taking $P = 5.7$ s as the minimum for SS Cyg yields $M_1(1) = 1.18$.

4.2 OY Car

Optical DNOs in the SU UMa star OY Car, in the period range of 19.4–28.0 s, were observed by Schoembs (1986) at the end of a superoutburst as the star fell from 12.9 to 14.4 magnitude (at maximum OY Car has $V(\text{supermax}) \simeq 11.5$, and at quiescence $V \sim 15.5$). Marsh & Horne (1998; hereafter MH) observed 18 s DNOs in OY Car using the HST at the very end of a superoutburst, just before it reached quiescent magnitude and therefore at a similar stage to the prominent DNOs seen in VW Hyi. Important aspects of these DNOs are (a) the presence of two periods with amplitudes 8–20 percent, at 17.94 s and 18.16 s, the former being sinusoidal, the latter being weaker but having a first harmonic with amplitude larger than that of its fundamental; (b) flux distributions of the oscillating components that are very much hotter than the average spectrum, and the first harmonic of the 18.16 s modulation is hotter than its fundamental; (c) eclipse of the oscillations that is total and occurs during the orbital phase range ± 0.03 , rather than the range ± 0.075 seen in the optical DNOs (Schoembs 1986), showing that the 1100–2500 Å oscillation flux is concentrated near the centre of the disc.

The duration of the eclipse of the HST oscillations at 17.94 s and the 9.07 s harmonic in OY Car is the same as that of the primary as measured at optical wavelengths (Wood et al. 1989) and of the X-ray eclipse in quiescence (Pratt et al. 1999). This demonstrates that the oscillatory components are all produced very close to the surface of the primary.

Our interpretation of these observations is similar to that for VW Hyi. The 17.94 s modulation is the rotation period of the equatorial belt of VW Hyi; the 18.16 s period is the result of the 17.94 s rotating beam being processed by a thickening of the inner disc rotating progradely with a period of 1480 s. The short eclipse duration of the processed component specifically requires the processing site to be close to the primary and not at the outer edge of the accretion disc. The first harmonic modulation, at 9.07 s period, is either the result of two accretion zones being visible to the thickened annulus of the disc, but not directly to us, or is due to the irregular shape of the processing blob.

A prediction of this model, in analogy with VW Hyi, is that QPOs with a period ~ 1500 s may occur in the light curve of OY Car at the end of outburst. The HST observation made by MH had a duration of only ~ 2250 s and therefore (in the presence of eclipses and other orbital modulation) was unsuitable for detection of such a QPO. However, the XMM-Newton X-ray observations of OY Car obtained by Ramsay et al. (2001) about two days after a normal outburst showed a ~ 2240 s modulation characteristic of obscuration of a central source by material circulating periodically above the plane of the accretion disc, having large amplitude in the 0.1–1.0 keV range but no detectable modulation in 1.0–10.0 keV. This may be a longer period evolution from an earlier ~ 1500 s modulation.

Occasional dips in the optical light curve of OY Car have been observed late in outburst (Schoembs 1986) and in quiescence (Schoembs, Dreier & Barwig 1987) that probably arise from obscuring matter, but no periodicities have been determined with any certainty. However, as Schoembs et al. pointed out, the dips in OY Car at minimum resemble

those in WZ Sge – for which we have a new interpretation based on our model for VW Hyi.

It is possible that the FeII curtains, seen in HST spectra of OY Car (Cheng et al. 2000) and in V2051 Oph, Z Cha and WZ Sge (Catalán et al. 1998), all of which possess DNOs, are the result of IP-like accretion curtains rotating with periods of tens of seconds.

4.3 WZ Sge

WZ Sge is an SU UMa type dwarf nova with superoutbursts occurring two or three decades apart. Brightness modulations at 28.952 s and 27.868 s in quiescence were discovered by Robinson, Nather & Patterson (1978), who found that in general either one or the other, but occasionally both were present. Many studies have been made of these oscillations, reviewed and extended in Patterson et al. (1998), with frequent claims that the 27.87 s oscillation and some associated sidebands are evidence for a rotating magnetic accretor (Patterson 1980; Warner, Tout & Livio 1996; Lasota, Kuulkers & Charles 1999). Important support for this model has come from the discovery of X-ray modulation at 27.87 s (Patterson et al. 1998), but analysis of HST observations (which also are dominated by the 27.87 s modulation) has shown that a simple magnetic accretor does not account for all of the observed periodicities (Skidmore et al. 1999), and that non-radial pulsation of the white dwarf primary could be a viable mechanism. Nevertheless, the observed rotation velocity of the primary in WZ Sge, $v \sin i = 1200 \text{ km s}^{-1}$ (Cheng et al. 1997b), together with $i = 70^\circ$ and $M_1(1) = 1.0 \pm 0.2$ (Cheng et al. 1997b; Spruit & Rutten 1998), gives $P(1) = 28 \pm 8 \text{ s}$, which is supportive of the model of rotational modulation from a magnetic accretor.

One of the problems with all models of the WZ Sge oscillations is the 28.95 s period, which does not appear related in any obvious way to the 27.87 s period and its optical sidebands. But by analogy with VW Hyi and OY Car we now have a simple explanation – which was first suggested in essence by Patterson (1980), but now we have a more clear idea of what a blob rotating in the disc consists of. Patterson’s idea was that the 28.95 s signal arises from a 27.87 s rotating beam processed by a blob revolving in the accretion disc at the beat period of $733 \pm 15 \text{ s}$. Lasota et al. (1999) claimed that to have such a period the reprocessing site would have to be far out in the disc and suggested the outer rim as a region that might be capable of exciting and sustaining QPOs.

We prefer, however, to adopt the VW Hyi model, with a QPO travelling wave in the *inner disc*. WZ Sge is unique, however, because it then becomes the only dwarf nova showing persistent DNOs and QPOs in quiescence. This implies a primary with a magnetic moment intermediate between those of normal dwarf novae and those of IPs, and also an accretion history that spun the primary up to its present rapid rotation rate. Again by analogy with VW Hyi it should be kept in mind that there may be an equatorial belt generating or enhancing the magnetic field and not firmly attached to the primary. That this is even probable is seen from the value of $P/\dot{P} \sim 1 \times 10^5 \text{ y}$ found for the 27.87 s oscillation in the 1976–1978 data by Patterson (1980), which is too short a time scale for it to involve the whole of the primary. Again in analogy with VW Hyi, no first harmonic of the 27.87 s

DNO is seen, but a harmonic of the reprocessed signal at 28.96 s is observed at 14.48 s (Provencal & Nather 1997).

Our QPO processing model for WZ Sge requires there to be a thickened region of the disc rotating progradely with a period of 744 s, which is the beat period of 28.952 s and 27.868 s. As well as processing radiation from the central source, this feature, when of sufficient amplitude, might be expected to obscure part of the central region in this high inclination system. We will demonstrate that this is in fact the case.

From the first light curves obtained for WZ Sge (Krzeminski & Kraft 1964) observers have commented on the presence of a dip of unknown origin in the light curve in the vicinity of orbital phase 0.3 (see, e.g., Fig 3.3 of Warner 1995a). The base level of this dip is often as deep, but rarely much deeper, than the minimum in the WZ Sge light curve which gives it its unusual “double hump” or W UMa-like profile. The dip at phase ~ 0.3 is so prominent that, although other, lesser dips are present, the latter have not been taken notice of. However, armed with the expectation of repetitive dips spread 744 s apart, it is immediately obvious (a) that many of the published light curves have such dips (e.g. the upper light curve in Fig 3.3 of Warner 1995a) and (b) the reason that they are not conspicuous is because they do not, or cannot, occur near phase 0.5 where the light is already reduced by another cause.

We reproduce in Fig. 3 a light curve of WZ Sge obtained by Dr. J.H. Wood through a B filter on 19 August 1988 using the Stiening multichannel photometer on the 82-in reflector at the McDonald Observatory. The original light curve, at 1 s time resolution, has been binned to 10 s. In addition to the eclipses every 81.6 min there are minor dips appearing at all phases other than around 0.5. Even by eye there is a suggestion of periodicity. This is confirmed by the Fourier transform of the light curve, shown in Fig. 4, in which we have prewhitened the light curve at the two strongest periodic components (the first and third harmonics of the orbital period) and which shows a prominent peak at $742 \pm 1 \text{ s}$. No DNOs are detectable in this light curve, showing that the QPO exists independently of the presence of DNOs.

Our impression, inevitably subjective, is that Fig. 3 shows only recurring dips and not the peaks seen in VW Hyi. This is in accord with the expectation (Section 3.2.1) that reprocessing from the wall will be largely hidden by the primary in a high inclination system. In addition, the primary in WZ Sge is cool ($\sim 15000 \text{ K}$) and the accretion luminosity onto it is low, so relatively little radiation is available for reprocessing.

Much of the ‘noise’ on each side of the 742 s signal in Fig. 4 is sidebands generated by the severe amplitude modulation of the recurrent dip in Fig. 3. The signal itself is the average amplitude and is much smaller than the extreme depths of the dips. In our new interpretation of Fig. 3, all of the major features arise from eclipse, the broad dip at orbital phase 0.5, and QPO dips. There is very little short time scale flickering.

It is usually thought that, with the (possible) exception of WZ Sge, no dwarf novae have DNOs in quiescence. We draw attention to the Einstein hard X-ray observation of HT Cas in quiescence on 23 Jan 1980, which showed a significant period of 21.88 s and an equal amplitude first

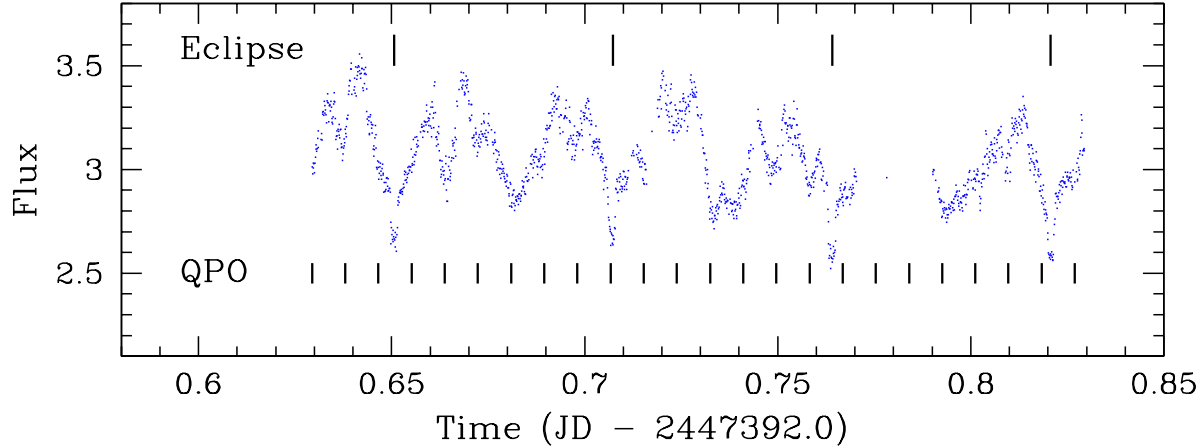


Figure 3. The light curve of WZ Sge, taken on 19 August 1988 by Dr. J.H. Wood. The eclipses are indicated by the upper vertical bars, and the QPO minima derived from the Fourier transform are marked by the lower bars.

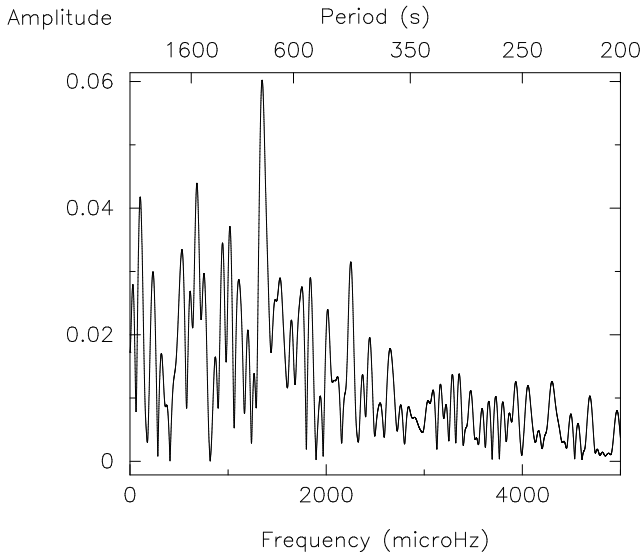


Figure 4. The Fourier transform of the light curve shown in Figure 3 after prewhitening. The highest peak is at 742 s.

harmonic (Cordova & Mason 1984). This is similar to the optical DNO periods seen during outburst. Warner (1995a) has pointed out that spectroscopic observations of HT Cas in quiescence are suggestive of stream overflow and impact onto a magnetosphere.

4.4 UX UMa

Optical DNOs with periods near 29 s were discovered in the nova-like UX UMa by Warner & Nather (1972) and more extensively observed and analysed by Nather & Robinson (1974; hereafter NR). More recently UV DNOs have been discovered by Knigge et al. (1998a) with HST observations. A number of points relevant to the content of this paper can be extracted from the observations of UX UMa:

- In analysing the flux distribution and eclipse observations obtained by HST, Knigge et al. (1998b) found that

they could not get a good fit with standard theoretical discs. One option they point out, which improves the fit, is to truncate the disc by removing the inner regions out to a few white dwarf radii. This also improves the fits in the nova-like IX Vel (Long et al. 1994), which is another system showing ~ 26 s DNOs (Warner, O'Donoghue & Allen 1985). Such results are certainly compatible with the model of magnetically controlled accretion in the inner disc.

- Knigge et al. (1998a) found a large shift in DNO oscillation phase during eclipse, similar to that seen by NR. In fact, in the two HST eclipse observations the phase shift was more than 360° , suggesting that the mean period derived for the DNOs before eclipse had changed at some time through eclipse. There are steps in the O - C curve through and after eclipse that resemble the discontinuous jumps in period seen in TY PsA and VW Hyi.

- In the O - C curves of NR and the second eclipse of Knigge et al. (1998a) there are oscillations - with a quasi period ~ 650 s in the former and ~ 400 s in the latter (at the end of and after eclipse). These are on a time scale suggestive of modulation by reprocessing from a travelling blob.

- DNOs in UX UMa are not always present. Their absence could mean that although present they are hidden from view from our perspective, or it could be that an increase in \dot{M} has crushed the magnetosphere down to the surface of the white dwarf, or it could be the result of a slight decrease in \dot{M} , which results in an increase in r_0 and cessation of accretion onto the primary because of propelling or at least prevention of steady accretion. In principle, distinction between the last two could be obtained if there is found to be a correlation between EUV flux and presence of DNOs. The damming up of accretion in the inner disc of an IP leads to an instability (Spruit & Taam 1993) which can produce short-lived outbursts (Warner 1995c) of the kind seen in the nova-like RW Tri (Still, Dhillon & Jones 1995), and which may be used to infer magnetically-truncated discs. Again, it would be interesting to see if there is a minor outburst in the EUV at the end of a period of DNO absence.

4.5 V2051 Oph

Steehgs et al. (2001: hereafter S2001) have observed both continuum and spectral line modulations in V2051 Oph towards the end of a normal outburst (at $V \simeq 14.8$). Continuum oscillations at 56.12 s and its first harmonic at 28.06 s are interpreted as originating from the white dwarf primary. The length of the observation (35 min) was insufficient to determine whether this modulation has the typical period variation of a DNO, but an earlier observation of a 42 s period (Warner & O'Donoghue 1987) at a brighter phase ($V \simeq 13.2$) suggests that it does. A period of 29.77 s was also observed, which has a beat period of 488 s with the 28.06 s modulation. The absence of a sideband at 26.53 s shows that, as in our observation of VW Hyi (Figures 18 and 19 of Paper I), the longer period is a reprocessed signal from a blob moving with the period of 488 s. Evidently there are two accretion regions in the equatorial belt of V2051 Oph, which itself has a rotation period of 56.12 s.

Periods of 28.06 and 29.77 s (but not twice their values) were also observed in the Balmer lines. Their similar amplitudes result in an apparent almost 100 percent amplitude modulation at 488 s. There is a weak indication of the 488 s period (which we recognise as a QPO) in the continuum light curve which, if correctly identified, implies that the maximum of the Balmer line oscillations (i.e., the time when the 28.06 s and 29.77 s modulations are in phase) corresponds to minimum of the QPO.

V2051 Oph is a high inclination system ($i \simeq 83.5^\circ$: Baptista et al. 1998), which leads to strong back-front asymmetry in the system, obscuration of the inner parts of the accretion disc by the primary, and the possibility of partial obscuration of the primary by a travelling wave in the inner disc. We would expect that the dominant continuum signal at $P(1)$ would result from reprocessing from the far side of the disc. Reprocessing from the travelling blob would also be seen at maximum advantage when the blob is on the far side except that it is partially obscured by the primary if the blob is in the inner region of the disc: taking $P(1) = 56$ s and $M_1(1) = 0.78$ (Baptista et al. 1998) gives $r_0 \simeq 3.0R(1)$ from equation 26, so by analogy with VW Hyi vertical thickening of the disc may be excited just beyond $r \sim 3R(1)$.

S2001 find a strong wavelength dependent phase shift across the emission line profile, in the sense that oscillation maximum moves from blue to red across the profile every 29.77 s. At the 28.06 s period no strong systematic effect is observed. There is similarity with what is seen in DQ Her, where the phase dependence has the opposite sign, i.e., the wavelength of maximum amplitude moves from red to blue across the profile (Chanan, Nelson & Margon 1978; Martell et al. 1995). In DQ Her the inclination is so great that only the far side of the disc is visible over the front edge of the disc, so a prograde rotating beam, as seen by us, can only illuminate material that is sequentially receding, moving transversely, and approaching, with little or no part of the return path visible. The earlier of these observations of DQ Her was very helpful in confirming the model of a rotating reprocessing beam.

The different behaviour in V2051 Oph can be interpreted as follows. The two rotating beams produce a 28.06 s signal from ionization and recombination of the axially symmetric part of the optically thin upper atmospheric regions

of the disc in its inner parts (i.e., just beyond r_0). Because of obscuration by the primary, and optical thickness effects in the material at radial velocity extrema (see below) there is not a clear or complete S-wave produced by spectra folded at this period (see Fig. 7 of S2001) – in particular, the passage of the S-wave from red to blue is reduced in intensity because of obscuration by the primary (e.g., at $r_0 = 3R(1)$, the Keplerian rotation is $v_0 \simeq 2200 \text{ km s}^{-1}$ and obscuration by the full diameter of the white dwarf would remove the return section of the S-wave for velocities in the range $+700 > v > -700 \text{ km s}^{-1}$). It should also be kept in mind that the illuminating beam may be very broad and therefore the profile of the reprocessed line emission will be broadened, asymmetric and have a velocity amplitude smaller than v_0 .

Reprocessing from the travelling blob is similarly affected: gas streams through the region of vertical thickening at the Keplerian velocity, the elevated highest regions will generate an emission line spectrum, and illumination by the beam generates a modulation at the 'synodic' period of 29.77 s. Because the region is optically thin in the visible, but the vertical density falls roughly exponentially, the largest emission measure will occur at a height where the gas first becomes optically thin. When the travelling wall is at inferior conjunction (i.e., 'back-lit' by the rotating beam) the axially symmetric component and the component from the blob are in phase, agreeing with the appearance of largest amplitude of the Balmer emission line modulation at QPO minimum. When the wall is at quadrature the larger physical path length in our direction will push the height of optical thinness higher, where the gas density and emission measure are lower, reducing the emission line intensity. This and the velocity-averaging effect of a broad illuminating beam and an extended blob, reduce the apparent velocity amplitude of the S-wave from the expected $\pm 2200 \text{ km s}^{-1}$. In Fig. 8 of S2001 the emission appears to extend to $\pm 1800 \text{ km s}^{-1}$. We feel, therefore, that a travelling wave at $\sim 3R(1)$ in the disc, rather than a blob moving at Keplerian velocity at $\sim 12R(1)$, as advocated by S2001, is compatible with the observations. It will certainly be easier to account for the readily visible ~ 29 s oscillations in the Balmer line flux if the reprocessing site is at $3R(1)$ than if it is at $12R(1)$.

Finally, we note the unusual light curve of run S3320 shown in Fig. 1 of Warner & O'Donoghue (1987). The dips in the first two thirds of this light curve, which was of V2051 Oph during outburst, resemble those in WZ Sge (Fig. 3). We suggest that there was a large amplitude QPO present, with a period near to one third of the orbital period (i.e., ~ 1800 s) which decayed steadily over the ~ 7.5 h duration of the run. We have confirmed that there were no DNOs in this run, although the 42 s DNO was present on the previous night. This is a further example of the independence of DNOs and QPOs.

4.6 V436 Cen

DNOs near 20 s period were found in V436 Cen during a superoutburst (Warner 1975) and analysed by Warner & Brickhill (1978). The period (obtained by periodogram analysis of successive sections of the light curve) varied cyclically over a range $\sim 19.3\text{--}20.3$ s. This effect has not been previously understood, but noting that there are QPOs present in the light curve (see Fig. 1 of Warner 1975) which have periods

in the range 400–500 s, we suggest that a ‘direct’ DNO with period ~ 19.3 s is sometimes dominant, and at other times its ‘reprocessed’ component at periods 20.1–20.3 s dominates. This will be analysed more completely elsewhere.

5 CONCLUDING REMARKS

The principal observational and interpretative points made in our two papers are:

- Optical DNOs over the range 14 – 40 s have been observed in VW Hyi outbursts – previously the shortest periods had been detected only in X-Ray observations.
- Over a time of about 12 hours at the end of outburst the DNOs in VW Hyi increase rapidly in period and then recover to shorter periods.
- QPOs are often present during outbursts. For the first time we have detected a significant evolution of QPO period as the luminosity at the end of outburst decreases.
- We develop the Low Inertia Magnetic Accretor model, in which accretion is taking place onto a weakly magnetic white dwarf, spinning up an equatorial band which thereby enhances the intrinsic magnetic field. In this way, magnetically channelled accretion can occur even on low field CV primaries.
- Frequent DNO period discontinuities are interpreted as magnetic reconnection events. The observed reduction of coherence in DNOs late in outburst is a consequence of the more rapidly changing rate of mass transfer through the inner disc, which causes the inner radius of the disc to move outwards, preventing an equilibrium (as in an intermediate polar) from being attained.
- Because the rate at which the inner disc radius moves outwards is greater than the equatorial belt can adjust to, there is an inevitable stage of “propeller” in which much of the accreting gas is centrifuged away from the primary. This corresponds to the observed phase of rapid deceleration of the DNOs. At this time, the rate of mass transfer onto the primary, as indicated by the EUV flux, falls almost to zero.
- The frequency doubling of DNOs observed in the EUV of SS Cyg is attributed to optical thickness and geometric effects that arise from the LIMA model.
- The QPO modulation is interpreted as a prograde travelling wave (or “wall”) near the inner edge of the disc. The luminosity variations come from obscuring and reprocessing of radiation from the central region of the disc (and primary), rather than as variations intrinsic to the disc oscillation itself. A possible excitation mechanism, associated with the magnetic reconnection mechanism, is proposed.
- The observed modulation of the DNOs at the QPO period – leading at times to a ‘QPO sideband’ – arises from interception of the rotating DNO beam by the travelling wall.
- Applied to other CVs, the models account for the pair of DNO frequencies observed in OY Car during outburst (MH), the persistent pair of DNOs seen in WZ Sge during quiescence (in which we demonstrate for the first time the existence of a QPO frequency which is the difference frequency of the DNOs), the pair of DNOs seen in V2051 during outburst (S2001), and the puzzling behaviour of DNOs seen in V436 Cen during outburst.

We have proposed that the QPOs are due to the interception of radiation by a travelling wall. In this connection the QPOs in SW UMa observed during a superoutburst (Kato, Hirata & Minishege 1992) are very informative. Near the minimum of each sinusoidal ~ 370 s modulation, where in our model the wall would be partially obscuring the inner disc, a dip of depth ~ 0.1 mag lasting for ~ 70 s was seen. The duration is appropriate for partial eclipse of the primary by the highest part of the travelling wall. Kato et al. (1992) suggest obscuration by a body of horizontal dimension $> 6 \times 10^9$ cm rotating at the Keplerian period, which would place it at $\sim 7.5 R(1)$. The orbital inclination of SW UMa is not known, but is believed to be $\sim 45^\circ$ (Warner 1995a). To obscure the primary would therefore require a vertical thickening $\gtrsim 7 \times 10^9$ cm. We suggest that a QPO wall at a radial distance of the disc $\sim 1.5 R(1)$ and vertical height $\sim 1 \times 10^9$ cm would be a more realistic proposition.

A deeply eclipsing CV with large amplitude QPOs is required to help locate the radial distance of the travelling wall. Unfortunately WZ Sge does not satisfy this requirement (Fig. 3) because there are other modulations that affect the shape of eclipse and make interpretation difficult.

The possible success of the LIMA model developed here is seen as evidence for CV primaries with magnetic fields weaker than those of IPs – an extension to $B \lesssim 1 \times 10^5$ G, where the field is not strong enough to lock the envelope to the interior, but is powerful enough to cause some channelled accretion flow. Isolated white dwarfs exist with $B < 10^5$ G (Schmidt & Smith 1994) so we can expect CV primaries also to be represented at this level. Such weak fields are currently not measurable directly, but the DNO phenomena provide indirect evidence for their existence.

That some parameter, taking different values in different systems, lives in CVs is seen from the fact that otherwise similar CVs can have strong or absent DNOs. In our interpretation this parameter is $B(1)$, and the latter stars have small or zero values of it. Variations of $B(1)$, and \dot{M} , and differences of $M(1)$, combine to produce the range of DNO phenomena. The apparent absence of DNOs in any IP is in accord with the LIMA model – fields strong enough to generate the canonical IP behaviour should prevent slippage of the equatorial belt. Similarly, we would not expect a hot equatorial belt to be observed after an outburst of an IP.

Not all high \dot{M} discs show QPOs, again showing the existence of a hidden parameter – which might again be $B(1)$ and the ability to excite waves in the disc.

It has not escaped our notice that the DNO and QPO phenomena described here have apparent analogues among the accreting neutron stars. For example, the behaviour of the O–C diagram for the ~ 5 Hz QPOs in the Rapid Burster (Dotani et al. 1990) is similar to that in CVs. The kHz DNOs and their companions at not quite constant frequency difference (e.g. van der Klis 2000) resemble the double DNOs in VW Hyi, OY Car and WZ Sge. The frequencies depend on luminosity, as in CVs. Furthermore, the VW Hyi QPO/DNO period ratio of ~ 15 (Figure 3 of Paper I) is the same as that seen in X-ray binaries – indeed, our VW Hyi data fit on an extrapolation of Figure 2 of Psaltis, Belloni & van der Klis (1999) to frequencies two orders of magnitude lower than seen in the X-ray systems. This area, where similar phenomena appear, separated by the gravitationally determined ratio of time scales $(\bar{\rho}_{ns}/\bar{\rho}_{wd})^{1/2}$, remains to be explored.

ACKNOWLEDGMENTS

Part of this work was carried out while BW was visiting the Astrophysics Groups at Keele University and the Australian National University. He expresses his gratitude to both for their support and hospitality. Financial support for this work came from the University of Cape Town. We are grateful to the anonymous referee for suggestions that have led to improvements of presentation of this and Paper I.

REFERENCES

- Allan A., Hellier C., Beardmore A., 1998, *MNRAS*, 295, 167
 Baptista R., Catalan M.S., Horne K., Zilli D., 1998, *MNRAS*, 300, 233
 Belloni T., Verbunt F., Beuermann K., Bunk W., Izzo C., Kley W., Pietsch W., Ritter H., Thomas H.-C., Voges W., 1991, *A&A* 246, L44
 Bruch A., 1992, *A&A*, 266, 237
 Cannizzo J.K., 1993, *ApJ*, 419, 318
 Carroll B.W., Cabot W., McDermott P.N., Savedoff M.P., van Horn H.M., 1985, *ApJ*, 296, 529
 Catalán M.S., Horne K., Cheng F.H., Marsh T.R., Hubeny I., 1998, in Howell S., Kuulkers E., Woodward C., eds., *ASP Conf. Ser. Vol. 137, Wild Stars in the Old West*. Astron. Soc. Pac., San Francisco, p. 426
 Chanan G.A., Nelson J.E., Margon B., 1978, *ApJ*, 226, 963
 Cheng F.H., Sion E.M., Horne K., Hubeny I., Huang M., Vrtilík S.D., 1997a, *AJ*, 114, 1165x
 Cheng F.H., Sion E.M., Szkody P., Huang M., 1997b, *ApJ*, 484, L149
 Cheng F.H., Horne K., Marsh T.R., Hubeny I., Sion E.M., 2000, *ApJ*, 542, 1064
 Choi C.-S., Dotani T., Agrawal P.C., 1999, *ApJ*, 525, 399
 Cordova F.A., Mason K.O., 1984, *MNRAS*, 206, 879
 Cordova F.A., Chester T.J., Tuohy I., Garmire G.P., 1980, *ApJ*, 235, 163
 de Jager O.C., Meintjes P.J., O'Donoghue D., Robinson E.L., 1994, *MNRAS*, 267, 577
 Dotani T., Mitsuda K., Inoue H., Tanaka Y., Kawai N., Tawara Y., Makishima K., van Paradijs J., Penninx W., van Der Klis M., Tan J., Lewin W.H.G., 1990, *ApJ*, 350, 395
 Durisen R.H., 1973, *ApJ*, 183, 215
 Eracleous M., Horne K., Robinson E.L., Zhang E.-H., Marsh T.R., Wood J.H., 1994, *ApJ*, 433, 313
 Gänsicke B.T., Beuermann K., 1996, *A&A*, 309, L47
 Ghosh P., Lamb F.K., 1978, *ApJ*, 223, L83
 Ghosh P., Lamb F.K., 1979, *ApJ*, 234, 296
 Harrison T.E., McNamara B.J., Szkody P., McArthur B.E., Benedict G.F., Klemola A.R., Gilliland R.L., 1999, *ApJ*, 515, L93
 Hartmann H.W., Wheatley P.J., Heise J., Mattei J., Verbunt F., 1999, *A&A*, 349, 588
 Hellier C., 1996, *IAU Colloq. No. 158*, 143
 Hildebrand R.H., Spillar E.J., Middleditch J., Patterson J., Stiening R.F., 1980, *ApJ*, 238, 145L
 Hoare M.G., Drew J.E., 1991, *MNRAS*, 249, 452
 Huang M., Sion E.M., Hubeny I., Cheng F.H., Szkody P., 1996, *ApJ*, 458, 355
 Jones M.H., Watson M.G., 1992, *MNRAS*, 257, 633
 Kato T., Hirata R., Mineshige S., 1992, *PASJ*, 44, 215L
 Katz J.I., 1975, *ApJ*, 200, 298
 Kawaler S.D., 1988, *ApJ*, 333, 236
 Knigge C., Drake N., Long K.S., Wade R.A., Horne K., Baptista R., 1998a, *ApJ*, 499, 429
 Knigge C., Long K.S., Wade R.A., Baptista R., Horne K., Hubeny I., Rutten R.G.M., 1998b, *ApJ*, 499, 414
 Krzeminski W., Kraft R.P., 1964, *ApJ*, 140, 921
 Lamb D.Q., 1988, in Coyne G.V., et al., eds., *Polarized Radiation of Circumstellar Origin*. Vatican Observatory, Vatican, p. 151
 Lamb D.Q., Masters A.R., 1979, *ApJ*, 234, 117L
 Lamb F.K., Aly J.-J., Cook M.C., Lamb D.Q., 1983, *ApJ*, 274, 71L
 Lasota J.-P., Kuulkers E., Charles P., 1999, *MNRAS*, 305, 473
 Livio M., Pringle J.E., 1992, *MNRAS*, 259, 23P
 Long K.S., Blair W.P., Bowers C.W., Davisen A.F., Kriss G.A., Sion E.M., Hubeny I., 1993, *ApJ*, 405, 327
 Long K.S., Wade R.A., Blair W.P., Davidsen A.F., Hubeny I., 1994, *ApJ*, 426, 704
 Long K.S., Blair W.P., Hubeny I., Raymond J.C., 1996, *ApJ*, 466, 964
 Lubow S.H., 1989, *ApJ*, 340, 1064
 Lubow S.H., Pringle J.E., 1993, *ApJ*, 409, 360 (LP)
 Lubow S.H., Shu F.H., 1975, *ApJ*, 198, 383
 Marsh T.R., Horne K., 1998, *MNRAS*, 299, 92 (MH)
 Martell P.J., Horne K., Price C.M., Gomer R.H., 1995, *ApJ*, 448, 380
 Mauche C.W., 1996a, *ApJ*, 463, 87L
 Mauche C.W., 1996b, in Bowyer S., Malina R.F., eds., *Astrophysics of the Extreme Ultraviolet*. Kluwer, Dordrecht, p. 317
 Mauche C.W., 1997, in Wickramasinghe D.T., et al., eds., *ASP Conf. Ser. Vol. 121, Accretion Phenomena and Related Outflows*. Astron. Soc. Pac., San Francisco, p. 251
 Mauche C.W., 1998, in Howell S., Kuulkers E., Woodward C., eds., *ASP Conf. Ser. Vol. 137, Wild Stars in the Old West*. Astron. Soc. Pac., San Francisco, p. 113
 Mauche C.W., Mattei J., Bateson F., 2001, in Podsiadlowski P., et al., eds., *Evolution of Binary & Multiple Star Systems*. Bormio, Italy
 Mauche C.W., Wade R.A., Polidan R.S., van der Woerd H., Paerels F.B.S., 1991, *ApJ*, 372, 659
 Mestel L., 1953, *MNRAS*, 113, 716
 Narayan R., Popham R., 1993, *Nature*, 362, 820
 Nather R.E., Robinson E.L., 1974, *ApJ*, 190, 637 (NR)
 Nauenberg M., 1972, *ApJ*, 175, 417
 Norton A.J., Beardmore A.P., Allan A., Hellier C., 1999, *A&A*, 347, 203
 O'Donoghue D., 1986, *MNRAS*, 220, 23P
 Paczynski B., 1978, in Zytkow A., ed., *Nonstationary Evolution of Close Binaries*. Polish Scientific Publ., Warsaw, p. 89
 Patterson J., 1980, *ApJ*, 241, 235
 Patterson J., 1981, *ApJS*, 45, 517
 Patterson J., Richman H., Kemp J, Mukai K., 1998, *PASP*, 110, 403
 Petterson J., 1980, *ApJ*, 241, 235
 Popham R., 1999, *MNRAS*, 308, 979
 Pratt G., Hassall B.J.M., Naylor T., Wood J.H., 1999, *MNRAS*, 307, 413
 Pringle J.E., Savonije G.J., 1979, *MNRAS*, 187, 777
 Pringle J.E., Bateson F.M., Hassall B.J.M., Heise J., Holberg J.B., Polidan R.A., van Amerongen S., van der Woerd H., van Paradijs J., Verbunt F., 1987, *MNRAS*, 225, 73
 Provencal J.L., Nather R.E., 1997, *Astrophys.Sp.Sci.Libr.*, 214, 67
 Psaltis D., Belloni T., van der Klis M., 1999, *ApJ*, 520, 262
 Ramsay G., Poole T., Mason K., Córdoba F., Friedhorsky W., Breeveld A., Much R., Osborne J., Pandel D., Potter S., West J., Wheatley P., 2001, *A&A*, 365, 288L
 Robinson E.L., Nather R.E., Patterson J., 1978, *ApJ*, 219, 168
 Robinson E.L., Zahng E.-H., Stover R.J., 1986, *ApJ*, 305, 732
 Schmidt G.D., Smith P.S., 1994, *ApJ*, 423, 63
 Schoembs R., 1986, *A&A*, 158, 233
 Schoembs R., Dreier H., Barwig H., 1987, *A&A*, 181, 50
 Sion E.M., 1995, *ApJ*, 438, 876

- Sion E.M., Cheng F.H., Huang M., Hubeny I., Szkody P., 1996, ApJ, 471, L41
- Skidmore W., Welsh W.F., Wood J.H., Catalan M.S., Horne K., 1999, MNRAS, 310, 750
- Spruit H.C., Rutten R.G.M., 1998, MNRAS, 299, 768
- Spruit H.C., Taam R.E., 1993, ApJ, 402, 593
- Steeghs D., O'Brien K., Horne K., Gomer R., Oke J.B., 2001, MNRAS, in press (S2001)
- Stiening R.F., Hildebrand R.H., Spillar E.J., 1979, PASP, 91, 384
- Still M.D., Dhillon V.S., Jones D.H.P., 1995, MNRAS, 273, 849
- Szkody P., Hoard D.W., Sion E.M., Howell S.B., Cheng F.H., Sparks W.M., 1998, ApJ, 497, 928
- Uzdensky D.A., Konigl A., Litwin C., 2001, ApJ, in press
- van der Klis M., 2000, ARA&A, 38, 717
- van der Woerd H., Heise J., 1987, MNRAS, 225, 141
- van der Woerd H., Heise J., Paerels F., Beuermann K., van der Klis M., Motch C., van Paradijs J., 1987, A&A, 182, 219
- van Teeseling A., 1997, A&A, 324, 73
- Wang Y.-M., 1996, ApJ, 465, L111
- Warner B., 1975, MNRAS, 173, 37P
- Warner B., 1987, MNRAS, 227, 23
- Warner B., 1995a, Cataclysmic Variable Stars, Cambridge Univ. Press, Cambridge
- Warner B., 1995b, in Buckley D.A.H., Warner B., eds., ASP Conf. Ser. Vol. 85, Cape Workshop on Magnetic Variables. Astron. Soc. Pac., San Francisco, p. 343
- Warner B., 1995c, Ap.Sp.Sci., 230, 83
- Warner B., Brickhill A.J., 1978, MNRAS, 182, 777
- Warner B., Nather R.E., 1972, MNRAS, 159, 429
- Warner B., O'Donoghue D., 1987, MNRAS, 224, 733
- Warner B., O'Donoghue D., Allen S., 1985, MNRAS, 212, 9P
- Warner B., O'Donoghue D., Wargau W., 1989, MNRAS, 238, 73
- Warner B., Tout C.A., Livio M., 1996, MNRAS, 282, 735
- Wheatley P.J., Verbunt F., Belloni T., Watson M.G., Naylor T., Ishida M., Duck S.R., Pfefferman E., 1996, A&A, 307, 137
- Wickramasinghe D.T., Wu K., Ferrario L., 1991, MNRAS, 249, 460
- Wood J.H., Horne K., Berriman G., Wade R., O'Donoghue D., Warner B., 1986, MNRAS, 219, 629
- Wood J.H., Horne K., Berriman G., Wade R., 1989, ApJ, 341, 974
- Woudt P.A., Warner B., 2002, MNRAS, in press (Paper I)
- Wynn G.A., King A.R., Horne K., 1997, MNRAS, 286, 436